



# Superior electrochemical properties of manganese dioxide/reduced graphene oxide nanocomposites as anode materials for high-performance lithium ion batteries



Suk-Woo Lee<sup>a</sup>, Chang-Wook Lee<sup>a</sup>, Seung-Beom Yoon<sup>a</sup>, Myeong-Seong Kim<sup>a</sup>,  
Jun Hui Jeong<sup>a</sup>, Kyung-Wan Nam<sup>b</sup>, Kwang Chul Roh<sup>c,\*</sup>, Kwang-Bum Kim<sup>a,\*\*</sup>

<sup>a</sup> Department of Material Science and Engineering, Yonsei University, 134 Shinchon-dong, Seodaemun-gu, Seoul 120-749, Republic of Korea

<sup>b</sup> Department of Energy and Materials Engineering, Dongguk University, 30, Pildong-ro 1gil, Jung-gu, Seoul 100-715, Republic of Korea

<sup>c</sup> Energy Efficient Materials Team, Energy & Environmental Division, Korea Institute of Ceramic Engineering & Technology, 101 Soho-ro, Jinju-si, Gyeongsangnam-do 660-031, Republic of Korea

## HIGHLIGHTS

- MnO<sub>2</sub>/rGO nanocomposites were synthesized via a simple solution method using CTAB.
- MnO<sub>2</sub>/rGO nanocomposites have a large specific surface area and mesoporous structure.
- GITT revealed that MnO<sub>2</sub>/rGO nanocomposites have superior kinetic properties.
- Unique structural properties provide superior rate capability and cyclability.

## ARTICLE INFO

### Article history:

Received 16 December 2015

Received in revised form

13 February 2016

Accepted 15 February 2016

### Keywords:

Lithium ion batteries

Manganese dioxide

Reduced graphene oxide

Nanocomposite

High-performance anode materials

Energy efficiency

## ABSTRACT

MnO<sub>2</sub>/reduced graphene oxide (rGO) nanocomposites were synthesized via a simple solution method at room temperature for use in Li-ion batteries. Owing to the mesoporous features as well as the high electrical conductivity of rGO, the overall electronic and ionic conductivities of the nanocomposite were increased, resulting in improved electrochemical properties in terms of specific capacity, rate capability, and cyclability. In particular, as-prepared nanocomposites showed 222 and 115 mAh g<sup>-1</sup> at a current density of as high as 5 and 10 A g<sup>-1</sup>, and the specific capacitance was well maintained after 400 cycles. In addition, MnO<sub>2</sub>, via composite formation with rGO, permitted the additional conversion reaction between MnO and Mn<sub>3</sub>O<sub>4</sub>, resulting in the reduction of the initial irreversible capacity despite the high first discharge capacity caused by the large specific surface area.

© 2016 Elsevier B.V. All rights reserved.

## 1. Introduction

Lithium-ion batteries (LIBs) with high energy density have attracted considerable research attention owing to the increasing demand for compact and long-life electronic devices [1,2]. To obtain high-performance LIBs, electrode materials with high specific capacity and satisfactory cycle life are essential [3]. Among various potential electrode materials, transition metal oxides such as TiO<sub>2</sub>

[4–7], Fe<sub>3</sub>O<sub>4</sub> [8–10], SnO<sub>2</sub> [11–13], and Co<sub>3</sub>O<sub>4</sub> [14–17] have been studied widely owing to their high theoretical capacity (>700 mAh g<sup>-1</sup>) based on the conversion reaction and natural abundance of anode materials in a LIB. In particular, manganese dioxide (MnO<sub>2</sub>) has attracted much attention owing to its high theoretical capacity (1230 mAh g<sup>-1</sup>), low cost, and eco-friendliness. However, simplex MnO<sub>2</sub> electrodes suffer from low electrical conductivity and volume expansion and aggregation during cycling, resulting in poor rate capability and rapid capacity fading. In addition, their low initial efficiency limits practical applications [18–20]. To overcome these problems, carbonaceous materials with high electrical conductivity and adequate ductility have been

\* Corresponding author.

\*\* Corresponding author.

E-mail addresses: [rkc@kicet.re.kr](mailto:rkc@kicet.re.kr) (K.C. Roh), [kbkim@yonsei.ac.kr](mailto:kbkim@yonsei.ac.kr) (K.-B. Kim).

widely employed as matrices in metal oxides to improve their cycle performance [21–33].

Graphene, with a two-dimensional honeycomb  $sp^2$  carbon lattice, has attracted considerable attention owing to its properties and potential applications in many fields such as lithium batteries [34], sensors [35], supercapacitors [36], and hydrogen storage [37]. Among various carbon nanostructures, graphene is expected to be an excellent template for nanocomposites as LIB anodes owing to its superior electrical conductivity, large surface area, structural flexibility, and chemical stability [38–40].

In this light, a few studies have already focused on  $MnO_2$ /graphene composites for anode materials. For example, Li et al. reported an  $MnO_2$ /3D porous graphene-like composite (3D PG-Mn) with initial capacity of  $914 \text{ mAh g}^{-1}$  at a rate of  $100 \text{ mAh g}^{-1}$ ; the capacity sharply decayed to  $433 \text{ mAh g}^{-1}$  at a rate of  $1600 \text{ mA g}^{-1}$ , and capacity retention of 84.6% was reported after 200 cycles at  $100 \text{ mA g}^{-1}$  [30]. Sui et al. reported an  $MnO_2$ /nitrogen-doped graphene composite with reversible specific capacity of 1003 and  $636 \text{ mAh g}^{-1}$  at a rate of 100 and  $1500 \text{ mAh g}^{-1}$ , respectively [31]. Li et al. fabricated a graphene-wrapped  $MnO_2$ -graphene nanoribbon composite in which graphene flakes tightly sandwiched nanosized  $MnO_2$  that grew directly on the graphene nanoribbons; this nanocomposite showed specific capacity of  $672 \text{ mAh g}^{-1}$ , and the capacity decreased to  $300 \text{ mAh g}^{-1}$  at a rate of  $1000 \text{ mA g}^{-1}$  [32]. Yu et al. synthesized a free-standing layer-by-layer graphene- $MnO_2$  thin film that showed specific capacity of  $686 \text{ mAh g}^{-1}$  at a rate of  $100 \text{ mA g}^{-1}$  and capacity retention of 72% after 40 cycles with varying current rates from 100 to  $1600 \text{ mA g}^{-1}$  [41]. Although these materials showed better electrochemical properties compared to bare  $MnO_2$  particles, they have limited rate capability and cyclability despite the low loading amount of  $MnO_2$  in the composites (i.e., <70 wt%) [30–32,41].

In this study, we report the fabrication of  $MnO_2$ /rGO composites via a simple solution method using cetyltrimethylammonium bromide (CTAB). Uniform adsorption of CTAB on the rGO surface led to the homogeneous deposition of  $MnO_2$ , and CTAB could prevent the direct redox reaction between carbon and  $MnO_4^-$  [42]. In the composite, rGO can provide a highly conductive structure with large surface area to support well-contacted  $MnO_2$  nanoparticles. In addition, it effectively enhances the mechanical strength of the nanocomposite during volume changes and suppresses the aggregation of  $MnO_2$  nanoparticles during Li ion insertion/extraction. This results in superior rate capability and cyclability despite the high  $MnO_2$  loading amount in the composite (i.e., 75 wt%). In addition, the smooth penetration of  $Li^+$  ions through mesopores and high electrical conductivity of the rGO template improved the kinetic properties and led to the additional conversion reaction between  $MnO$  and  $Mn_3O_4$  in the nanocomposite, resulting in the reduction of the initial irreversible capacity. In particular, we revealed the origin of the additional conversion reaction between  $MnO$  and  $Mn_3O_4$  in the  $MnO_2$ /rGO nanocomposite by using the galvanostatic intermittent titration technique (GITT).

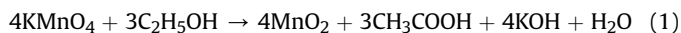
## 2. Experimental section

### 2.1. Preparation of rGO nanosheets

Graphite oxide (GO) was synthesized from purified natural graphite powder ( $\leq 45 \mu\text{m}$ , Aldrich) by a modified Hummers method as described previously [39]. rGO nanosheets were produced by a solid-state microwave irradiation method as reported previously [43]. Briefly, 90 wt% of GO powder was uniformly mixed with 10 wt% rGO powder using a ball-miller. The resulting GO/rGO mixture was placed in a quartz bottle and covered with a lid inside a glove box. The quartz bottle was filled with Ar gas in the glove box

to prevent the oxidation of carbon and then sealed tightly. The GO/rGO mixture in the quartz bottle was then placed in a microwave oven (Mars 5, CEM) and subjected to pulsed irradiation at 1600 W.

### 2.2. Synthesis of $MnO_2$ /rGO nanocomposite and bare $MnO_2$ nanoparticles



For preparing the  $MnO_2$ /rGO nanocomposite, CTAB (Aldrich) was used as a surfactant and protection layer to prevent direct contact between rGO and  $MnO_4^-$  ions. First, 43.5 mg of rGO was dipped into 1 wt% CTAB aqueous solution, and the solution was ultrasonicated to obtain a uniformly dispersed rGO/CTAB suspension. Next, 15 mL of 0.1 M  $KMnO_4$  solution was added to the rGO/CTAB suspension and stirred for 1 h. Then, ethanol was slowly added to the solution to reduce  $MnO_4^-$  ions to  $MnO_2$  until the purple color disappeared. The  $MnO_2$  formation mechanism is shown above in equation (1). After washing with ethanol, ammonium nitrate was added to remove residual  $CTA^+$  ions by ion exchange reaction between  $CTA^+$  ions and  $NH_4^+$  ions [44]. The final product was washed repeatedly with distilled water and ethanol and then dried at  $80^\circ\text{C}$  for 24 h. The detailed synthetic mechanism is reported in our previous research that reports the synthesis of  $MnO_2$ /CNT nanocomposites [45]. For comparison, bare  $MnO_2$  nanoparticles were similarly synthesized; 60 mL of ethanol was added to 150 mL of 0.01 M of  $KMnO_4$  aqueous solution and maintained at  $25^\circ\text{C}$  for 8 h under stirring. During the synthesis, the temperature of the solution was maintained at  $25^\circ\text{C}$  using a circulator.

### 2.3. Material characterization

X-ray diffraction (XRD, Rigaku,  $CuK\alpha$ , 40 kV, 20 mA) patterns were obtained in the  $2\theta$  range between  $10^\circ$  and  $80^\circ$  at intervals of  $4^\circ/\text{min}$  at room temperature. Raman spectroscopy (T64000, Jobin-Yvon) was also used to confirm the phase of  $MnO_2$ .  $N_2$  adsorption-desorption isotherms were measured using a Micromeritics ASAP ZORO instrument at 77 K, and the surface areas were calculated by the Brunauer–Emmett–Teller (BET) method.

The morphology of the as-prepared samples was characterized by transmission electron microscopy (TEM, JEM-ARM 200F). To determine the  $MnO_2$  content in the composite, TGA data were obtained using a thermal analysis instrument (TGA/DSC 1, Mettler Toledo) with a heating rate of  $10^\circ\text{C min}^{-1}$  under an air flow rate of  $50 \text{ mL min}^{-1}$ . Elemental analysis (EA) measurements were performed to quantify the carbon contents in the  $MnO_2$ /rGO nanocomposites.

### 2.4. Electrochemical test

The electrochemical properties were investigated using CR2032 coin-type cells that were assembled in an argon-filled glove box with lithium foils as the counter electrode and 1 M  $LiPF_6$  in ethylene carbonate and diethyl carbonate (EC:DMC, 1:1 in volume) as the electrolyte. The working electrode of the  $MnO_2$ /rGO nanocomposite was prepared by mixing 90 wt% of the active composite and 10 wt% of polyvinylidene difluoride (PVDF, Alfa Aesar) dissolved in N-methyl-2-pyrrolidone (NMP, Sigma–Aldrich) to form a slurry that was then coated on a copper foil substrate. For comparison, the electrode of bare  $MnO_2$  nanoparticles was fabricated with 10 wt% of binder and 22.5 wt% of carbon black. The carbon amount in both the  $MnO_2$ /rGO composite and the electrode made of bare  $MnO_2$  nanoparticles was the same. The mass loading and

Download English Version:

<https://daneshyari.com/en/article/1285459>

Download Persian Version:

<https://daneshyari.com/article/1285459>

[Daneshyari.com](https://daneshyari.com)